Int. J. Electrochem. Sci., 11 **(2016)** 291 - 302

International Journal of
ELECTROCHEMICAL
SCIENCE
www.electrochemsci.org

Corrosion Inhibition of Carbon Steel in acidic chloride medium by Cucumis Sativus (cucumber) Peel Extract

Ghadah M. Al-Senani

Chemistry Department, Science College, Princess Nora Bint Abdul Rahman University, Riyadh, KSA
E-mail: gmalsnany@pnu.edu.sa

Received: 1 October 2015 / *Accepted:* 9 November 2015 / *Published:* 1 December 2015

The corrosion inhibition of Cucumis sativus peel extract (*CSP*) on carbon steel in 1 M HCl solution was investigated by potentiodynamic polarization, and electrochemical impedance spectroscopy (EIS) techniques. The inhibition efficiency from potentiodynamic polarization and impedance measurements were agreement where the maximum inhibition is around 82%. The inhibition efficiency decreased as the temperature increased. The results obtained showed that *CSP* extract inhibited the corrosion process by a physical adsorption mechanism that followed the Langmuir adsorption isotherm models. The adsorption thermodynamic parameters that were calculated include, free energy of adsorption ($\Delta G°_{ads}$), activation energy (E_a), enthalpy of adsorption ($\Delta H°_{ads}$), and entropy of adsorption ($\Delta S°_{ads}$) revealed that the adsorption process are spontaneous and endothermic. All the results show that the *CSP* extract can act as an inhibitor against the corrosion of carbon steel in the HCl medium.

Keywords: Carbon steel, Hydrochloric acid, Corrosion inhibition, Cucumis sativus, Adsorption.

1. INTRODUCTION

Carbon steel has great significant where is widely used in industrial applications such as industrial cleaning and processing of oil wells, so the researchers have interest to using alternatives to toxic chemical inhibitors and the search for non-toxic natural inhibitors to reduce corrosion of metals [1]. The use of inhibitors is one of the best ways to protect metals against corrosion caused by acid solutions such acid pickling and acid descaling. Thus, efforts are now directed towards the formulation of safe inhibitors, plant extracts have become important as eco-friendly, economical, readily available and renewable sources of effective corrosion inhibitors [2]. The inhibition characteristics of green inhibitors studied such as Coffee Ground [1] Ruta Graveolens [2] Murraya Koenigii [3] Watermelon Rind [4] Oxandra Asbeckii [5] Euphorbia Falcata [6] Osmanthus Fragran leaves [7] Punica Plant [8]

Henna [9] Ruta Graveolens [10] . Nonetheless, there is still a need for research on other plants can be used as inhibitors in industrial applications.

The objective of this study was to investigate the inhibitory effects of the Cucumis sativus peel (*CSP*) extracts as corrosion inhibitors for carbon steel in 1 M HCl. Potentiodynamic polarization curves and electrochemical impedance measurements were utilized, and adsorption isotherms and thermodynamic parameters were calculated and discussed.

2. EXPERIMENTAL

2.1. Specimen preparation

Tests were performed on carbon steel specimens with the following composition (in wt. %) C 0.1%, Mn 1.23%, Si 0.265%, S 0.004%, P 0.011%, Cr 0.008%, Cu 0.024%, Sa 0.0016%, Ni 0.0214%, Ti 0.017%, Al 0.035%, Nb 0.036%, Ca 0.002%, CEV 0.32% and Fe balance. Carbon steel circular strips of the same composition with an exposed area of 1 cm^2 were used. Before each test, the specimen were ground with 800 and 1200 grit grinding papers, cleaned by distilled water and acetone.

2.2. Preparation of plant extract

CSP were dried in an electric furnace for 10 – 20 min at 50ºC then ground to powder. *CSP* dried powder (5g) was mixed with 500 ml of 1 M HCl and refluxed at 50ºC for 2 h. The extract was cooled, and filtered, this extract was found to be 35% (wt.%) of the used *CSP* dry weight. The extract used as a natural corrosion inhibitor in 1 M HCl solution.

2.3. Fourier transform infrared spectroscopy (FT-IR)

A KBr pellet was made from the dried extract and was characterized using FT-IR (Nicolet's auxiliary experiment module - AEM, Omnic software).

2.4. Electrochemical measurements

Potentiodynamic polarization, and electrochemical impedance spectroscopy measurements were carried out using ACM instruments model 1783. The electrochemical cell consisted of a conventional three-electrode configuration with graphite as the counter electrode and a saturated calomel electrode (*SCE*) coupled with a Luggin-Haber capillary as the reference electrode. The tip of the Luggin capillary was very close to the surface of the working electrode in order to minimize the ohmic contribution.

The working electrode was cut from a carbon steel rod with a cross-sectional area of 1 cm^2 and embedded in a Teflon holder. It was immersed in tests solutions with and without inhibitor, and then the open circuit potential was measured after 10 minutes to attain the steady state. Potentiodynamic polarization studies were performed with a scan rate of 0.2 mVs^{-1} in the potential range of ± 250 mV proportional to the potential of corrosion. All the potentials were recorded with respect to the SCE.

Then, corrosion current density (I_{corr}) is determined from the intercept of extrapolated cathodic and anodic Tafel slopes. The inhibition efficiency ($\eta_{inh}\%$) was calculated using Eq. 1:

$$\eta_{inh}\% = \frac{I_{corr} - I_{corr(inh)}}{I_{corr}} \times 100 \qquad (1)$$

where I_{corr} and $I_{corr(inh)}$ are referred to as the corrosion current density without and with inhibitor, respectively.

EIS measurements were performed at corrosion potentials, E_{corr}, over a frequency range of 10 kHz to 10 mHz with an AC signal amplitude perturbation of 10 mV peak to peak. The inhibition efficiency ($\eta_{inh}\%$), was calculated using Eq. 2:

$$\eta_{inh}\% = \frac{R_{ct(inh)} - R_{ct}}{R_{ct(inh)}} \times 100 \qquad (2)$$

where R_{ct} and $R_{ct(inh)}$ are referred to as the charge transfer resistance without and with the addition of the inhibitor, respectively.

The experiments were performed for various parameters such as, extract concentration variation (20%, 30%, 40%, and 50%), and temperature variation (25, 40, 50,and 60).

3. RESULTS AND DISSCUSION

3.1. FTIR results of CSP extract

The important IR absorption bands of inhibitors are given in Fig. 1 and their respective FT-IR peaks are given in Table 1. These results showed that the inhibitors containing functional groups with P, S, O and N atoms attached to aromatic ring, which are usually in corrosion inhibitors [11-12].

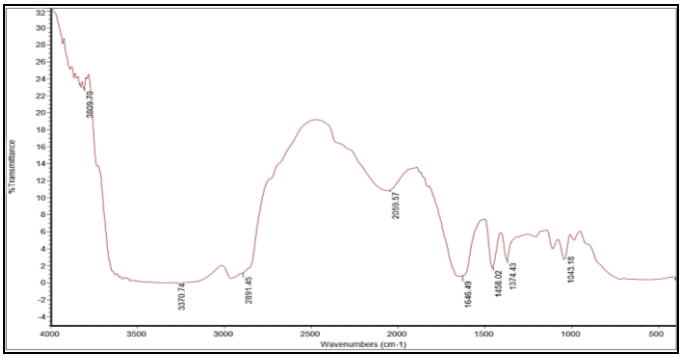

Figure 1. FTIR spectra of *CSP* extract.

Table 1. FT-IR peaks of CSP extract.

Peaks from FT-IR spectra	Possible functional groups
1043.18	P–O-C stretch / C–H stretch
1374.43	$–NO_2$
1458.02	$–SO_2–$ / –C–N–H
1646.49	C=N stretch
2059.57	C≡N stretch
2961.45	C–H (aromatic)
3370.74	NH_2 stretch
3809.70	N–C (aromatic)

3.2. Effect of CSP Concentration

3.2.1. Potentiodynamic polarization curves

The electrochemical parameters, anodic Tafel constant (β_a), cathodic Tafel constant (β_c), corrosion potential (E_{corr}), corrosion current density (i_{corr}), and the corresponding inhibition efficiencies for the corrosion of carbon steel in 1 M HCl solution without and with different concentrations (20% – 50%) of *CSP* at 25℃ are illustrated in Table 2. Moreover, Fig. 2 shows the anodic and cathodic potentiodynamic polarization curves for the previous tests. The CSP decrease the anodic and cathodic current densities as indicated in the potentiodynamic polarization curves which can be explained by the adsorption of organic compounds such as heteroatoms (oxygen, sulfur, phosphorus and nitrogen (found in CSP) at the carbon steel surface. Those aromatic rings or multiple bonds, found in organic compound acted as mixed type inhibitor [13]. It is clear from Table 2 that the Tafel slopes of the anodic (β_a) are significantly changed in the presence of CSP while very simple changed in the Tafel slopes of the cathodic (β_c) as result of adsorption the molecules of inhibitor. The corrosion process decrease as a result to both metallic dissolution and hydrogen evolution at the metal surface [14] the result in 1 M HCl solution 50% of *CSP* at 25℃ indicate decreased of The corrosion current density of carbon steel from 7.63 mA/cm to 1.32 mA/cm and increased in the corrosion inhibition efficiency to 82.70% this behavior is due to the good coverage of the metal surface by CSP molecules which blocked the reaction sites on the metal surface [13, 14].

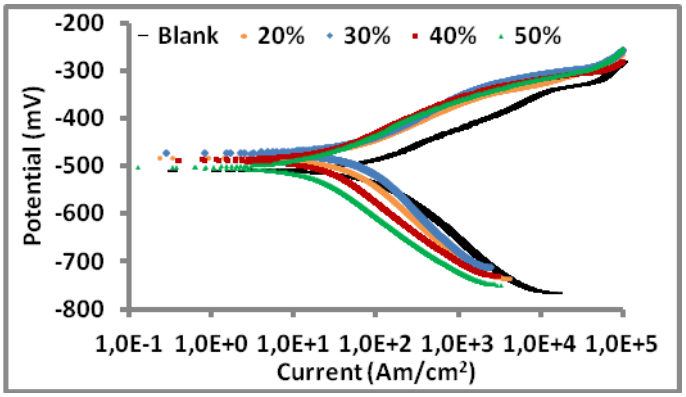

Figure 2. Potentiodynamic polarization curves for Carbon Steel in 1M HCl with and without 20, 30, 40 and 50% of CSP extract at 25ºC.

Table 2. Electrochemical parameters for Carbon Steel in 1M HCl with and without 20, 30, 40 and 50% of CSP extract at 25ºC.

C (g/ml)	E_{corr} (mV vs. SCE)	I_{corr} (mA cm^{-2})	β_c (mV)	β_a (mV)	C_{rate} (mm/year)	η_{inh}%
Blank	-510.59	7.63	144.50	87.80	87.80	0
20%	-484.74	4.51	140.73	58.81	51.89	40.90
30%	-500.14	2.20	134.57	57.75	25.28	71.21
40%	-504.31	1.70	127.02	56.46	19.56	77.72
50%	-505.44	1.32	113.89	54.44	15.25	82.70

3.2.2. Electrochemical impedance spectroscopy (EIS)

Fig. 3. shows the Nyquist plots for carbon steel in electrolyte solution in the absence and presence of various concentrations of *CSP* at 25ºC. The impedance spectra of carbon steel in HCl solutions with an inhibitor showed two capacitive loops as a result of the adsorption species like Cl^-_{ads} and H^+_{ads} on the metal surface in a process called relaxation process, or due to the adsorption of inhibitor on the metal surface or by the re-dissolution of the passive thin layer at low frequencies [4,5,15] which can be explained by the adsorption of the corrosion products on the metal surface such as $[FeOH]_{ads}$ and $[FeH]_{ads}$) [16]. This is manifested in the increase in R_{ct} values and with a simultaneous decrease in the values of C_{dl} (Table 3). The results suggests the adsorption of inhibitor molecules at the metal surface lead to the formation of a protective layer which increased the resistance in the charge transfer process at the electrode–electrolyte interface [6].

Following both the polarization and EIS studies, it was observed that inhibition efficiency increased with the increase in the concentration of *CSP* (Tables 2 and 3), that the active sites were almost blocked on the carbon steel surface under such condition. The efficiency of CSP was good compared to the previous studies like Coffee Ground extracts [1], Watermelon Rind extract [4] and Pipali (Piper longum) Fruit Extract [22].

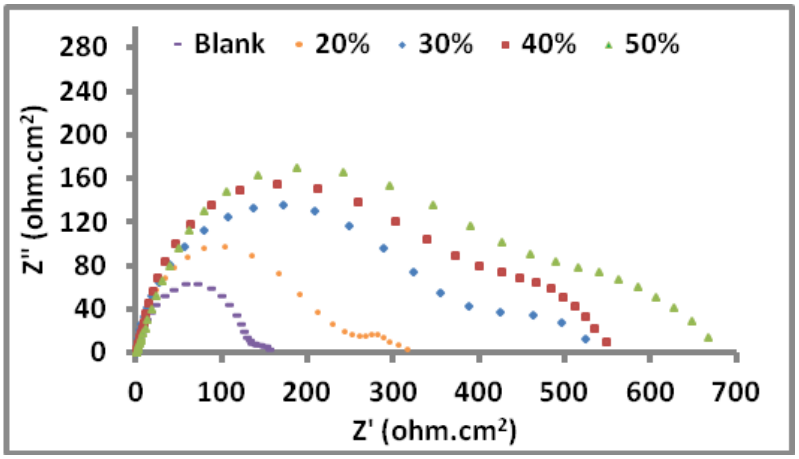

Figure 3. Electrochemical impedance spectra for Carbon Steel in 1M HCl with and without 20, 30, 40 and 50% of CSP extract at 25ºC.

Table 3. Impedance parameters for Carbon Steel in 1M HCl with and without 20, 30, 40 and 50% of CSP extract at 25ºC.

C (g/ml)	R_s (ohm.cm^2)	R_{ct} (ohm.cm^2)	Cdl (μF.cm^{-2})	I_{corr} (μA.cm^{-2})	η_{inh}%
Blank	7.53	116.4	56.41	224.10	0
20%	4.21	198.3	55.12	131.60	41.30
30%	3.72	388.8	50.80	67.10	70.06
40%	3.68	490.0	49.52	53.24	76.24
50%	2.43	592.1	48.94	44.06	80.34

3.3. Effect of Temperature

3.3.1. Potentiodynamic polarization

Potentiodynamic polarization studies in 1 M HCl in the absence and presence of 50% CSP (Figs. 4) and Table 4. showed an increased in the corrosion current density (I_{corr}) with the increase in temperature and a decreased in the corrosion inhibition efficiency with the increase in temperature. As a result of the dissolution of the metal and increase the development of hydrogen in the HCl solution without inhibitor and desorption of the some molecules physically adsorption on the carbon steel surface in case of the presence CSP.

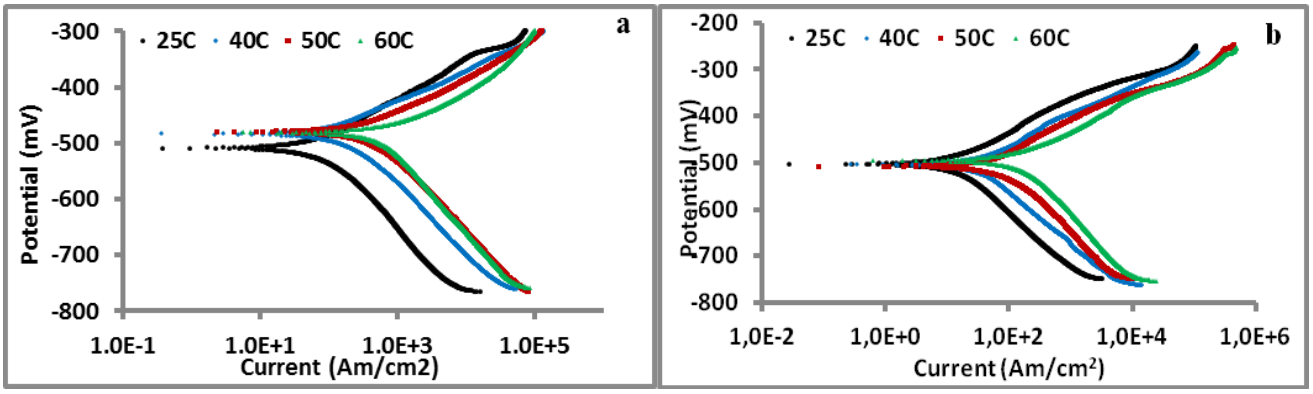

Figure 4. Potentiodynamic polarization curves for Carbon Steel in 1M HCl with and without 50% of CSP extract at 25, 40, 50 and 60ºC.

Table 4. Electrochemical parameters for Carbon Steel in 1M HCl with and without 50% of CSP extract at 25, 40, 50 and 60ºC.

Medium	TºC	E_{corr} (mV vs. SCE)	β_a (mV)	β_c (mV)	I_{corr} ($mA.cm^{-2}$)	C_{rate} (mm/year)	η_{inh}%
Blank	25	-510.59	87.80	144.50	7.63	87.80	-
	40	-485.36	66.19	117.61	10.16	116.99	-
	50	-480.44	70.62	129.19	13.08	150.51	-
	60	-482.26	57.64	135.20	16.70	192.20	-
CSP extract							
	25	-505.44	54.44	113.89	1.32	15.25	82.70
	40	-504.16	67.29	106.71	1.84	21.18	81.89
	50	-507.29	79.87	117.94	2.49	28.62	80.96
	60	-495.20	68.05	134.35	4.10	47.19	75.45

3.3.2. Electrochemical impedance spectroscopy (EIS)

A similar results has been obtained from the electrochemical impedance spectroscopy (EIS) and potentiodynamic polarization techniques regarding variation of the corrosion inhibition efficiency results obtained for the same tests, Nyquist plots obtained from EIS for carbon steel in 1 M HCl, in the absence and presence of 50% *CSP* at different temperatures are shown in Fig. 5. The diameter of the capacitive loop was observed to decrease as the temperature increased. This is manifested by the decrease in R_{ct} values with the simultaneous increase in the values of C_{dl} (Table 5). Both the polarization and EIS studies, showed that the effectiveness of the inhibitor decreased with increasing temperatures (Tables 4 and 5). The results can be explained in two ways first by the increase of the rate of the metal dissolution or by the shift of the adsorption/desorption equilibrium towards inhibitors desorption which lead to the reduce of the surface coverage.

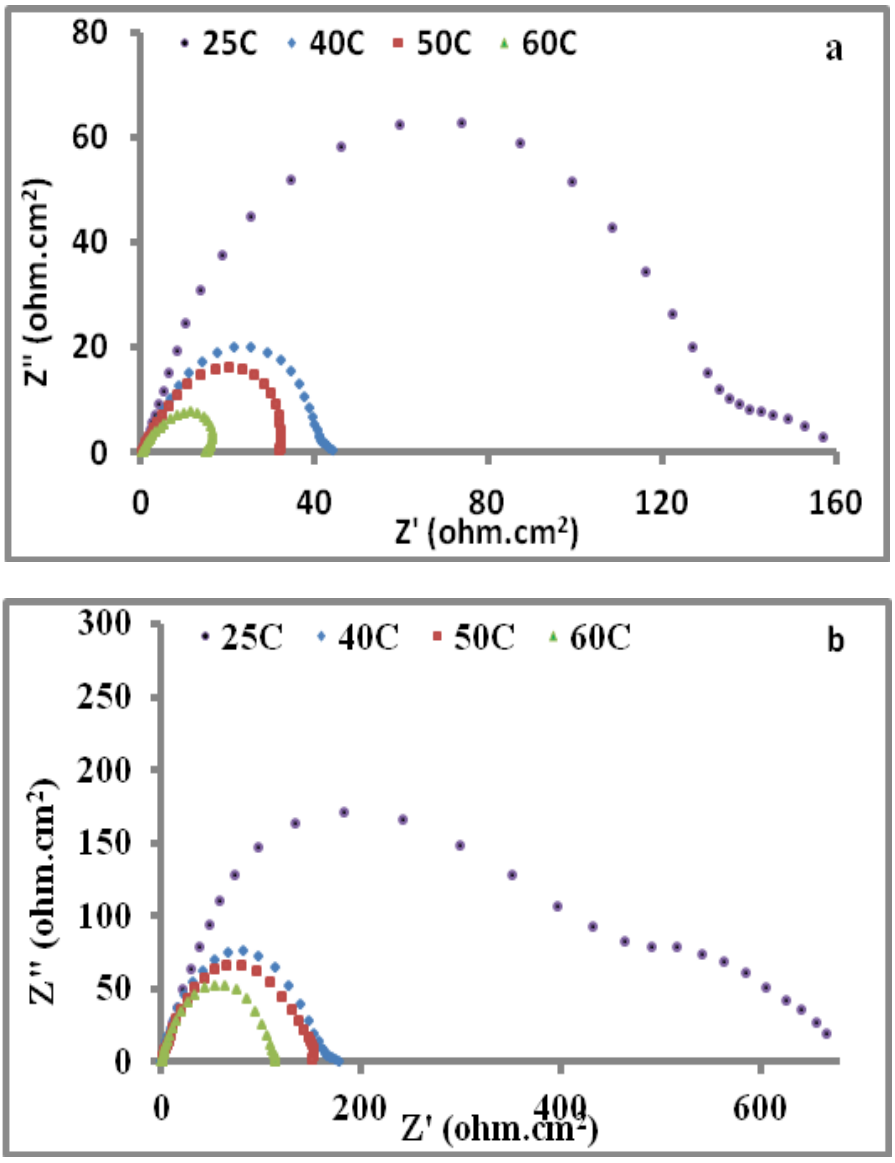

Figure 5. Electrochemical impedance spectra for Carbon Steel in 1M HCl with and without 50% of CSP extract at 25, 40, 50 and 60ºC.

Table 5. Impedance parameters for Carbon steel in 1 M HCl in (a) the absence and (b) presence of 50% aqueous *CSP* extract at various temperatures: 25, 40, 50 and 60ºC.

Medium	TºC	R_s (ohm.cm^2)	R_{ct} (ohm.cm^2)	Cdl (µF.cm^{-2})	I_{corr} (µA.cm^{-2})
Blank	25	7.53	116.4	56.41	224.10
	40	4.73	36.18	68.66	721.0
	50	4.99	27.34	42.58	954.2
	60	5.73	22.23	42.74	1174
CSP extract					
	25	2.43	592.1	48.94	44.06
	40	1.38	157.6	41.95	165.5
	50	1.46	128.5	45.07	203.0
	60	3.06	107.7	45.43	242.2

4. ADSORPTION ISOTHERM AND THERMODYNAMIC PARAMETERS

Adsorption isotherms are commonly used to understand the inhibition mechanism of the inhibitor molecules at the metal surface [6]. The fractional coverage values, θ, can be obtained from Eq. 3 [17] as follow:

$$\theta = \frac{R_{ct(inh)} - R_{ct}}{R_{ct(inh)}} \quad (3)$$

where R_{ct} and $R_{ct(inh)}$ are the charge transfer resistances without and with inhibitor, respectively.

Langmuir adsorption isotherm can be used to study the adsorption behavior of the plant extract on the carbon steel surface Eq. 4 [18-20]

$$\theta = \frac{K_{ads} C_{inh}}{1 + K_{ads} C_{inh}} \quad (4)$$

where C_{inh} is the inhibitor concentration, K_{ads} is the adsorption equilibrium constant.

Rearranging this Eq. 4 gives Eq. 5:

$$\frac{C_{inh}}{\theta} = \frac{1}{K_{ads}} + C_{inh} \quad (5)$$

The linear variation of C_{inh}/θ vs. C_{inh} of the *CSP* in 1 M HCl solutions showed that the adsorption is well fitted by the Langmuir adsorption isotherm (Fig. 6), the slope and R^2 presented in Table 6. The good correlation coefficient and the linearity appear at the plot suggest that the plot obeys Langmuir adsorption isotherm.

The R^2 values are very close to unity, indicating a strong agreement with Langmuir adsorption isotherm.

From the intercept of straight lines, K_{ads} values can be obtained and related to the free energy of adsorption, ΔG_{ads} by Eq. 6 [17]:

$$\Delta G^0_{ads} = -RT\ln(55.5\ K_{ads}) \quad (6)$$

where R is the universal gas constant, T is the absolute temperature and 55.5 is the molar heat of adsorption of water. The values of free energy of adsorption, $\Delta G°_{ads}$, are negative (Table 5), the negative value of $\Delta G°_{ads}$ indicates spontaneous adsorption process and the a high stability of the

adsorbed layer on the carbon steel surface. The value of - ΔG°ads is more than 20 kJ/mol due to strong the adsorbing inhibitor molecules on the carbon steel surface, which involves an electrostatic interaction between the atoms/ions on the metal surface and the adsorbed molecules [21]. This is a result of a mixed adsorption which involves a physical adsorption and chemical adsorption. Generally, the values of $\Delta G°_{ads}$ of up to -20 kJ/mol are consistent with electrostatic interaction between charged inhibitor molecules and the carbon steel surface (physical adsorption) and those more than -40 kJ/mol involves charge sharing or transfer from the inhibitor molecule to carbon steel surface to form a coordinate bond (chemisorption).

The Langmuir isotherm being followed confirms a mixed adsorption mechanism owing to the spontaneity of the process. Thus, the *CSP* extract can be used to inhibit the carbon steel corrosion in 1 M HCl.

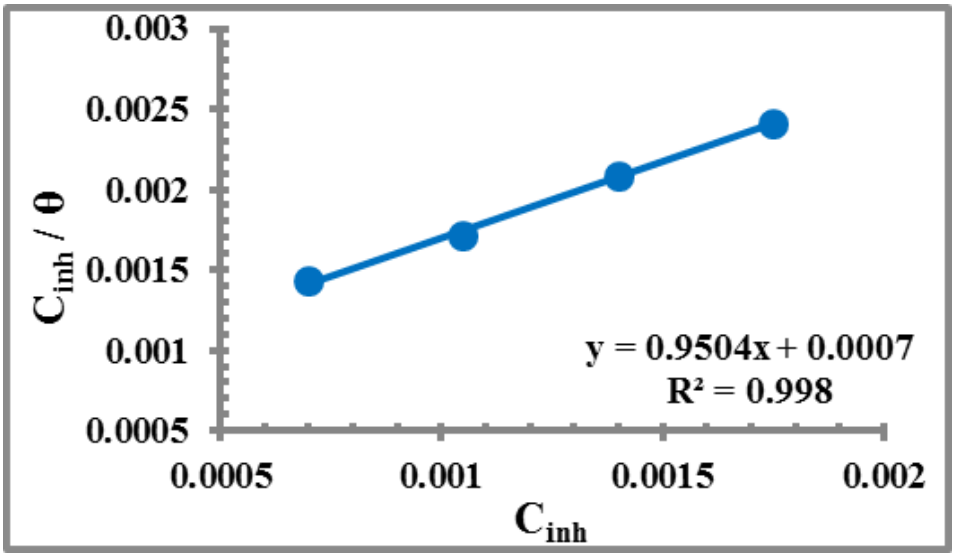

Figure 6. Langmuir isotherm plote for the CSP extract adsorbed on the Carbon Steel surface.

Table 6. Langmuir isotherm parameters for the CSP extract adsorbed on the Carbon Steel surface.

Slope	Intercept	R^2	K_{ads}	$\Delta G°_{ads}$ (KJ/mol)
0.950	0.0007	0.998	1428.57	- 27.95

The activation energy can be calculated from Eq. 7:

$\ln i_{corr} = \ln A - E_a/RT$ (7)

From Fig. 7a the slope $-E_a / R$ was obtained by plotting the $\ln i_{cor}$ of 1 M HCl in the absence and presence of 50% *CSP* versus 1/T. The calculated activation energies, E_a, and pre-exponential factors, A, are listed in Table 7. The high value of the apparent activation energy (E_a) in the presence of an inhibitor indicate that the adsorption of the inhibitor is physically adsorbed on the metal surface [7, 22].

The enthalpy of activation ($\Delta H°_{ads}$) and the entropy of activation ($\Delta S°_{ads}$) for the corrosion of carbon steel in 1 M H Cl solution in the absence and presence of *CSP* were calculated from the Arrhenius equation:

$$ln\left[\frac{I_{cor}}{T}\right] = ln\left[\frac{R}{Nh}\right] + \left[\frac{\Delta S°_{ads}}{R}\right] - \left[\frac{\Delta H°_{ads}}{R}\right] \quad (8)$$

where h is the Plank's constant (6.626176×10^{-34}Js) and N the Avogadro's number ($6.02252\times1023 mol^{-1}$). A plot of lni_{cor}/T versus 1/T gave a straight line (Fig. 7b) with a slope of $\Delta H°_{ads}/R$ and an intercept of $ln(R/Nh) + \Delta S°_{ads}/R$, from which the values of $\Delta S°_{ads}$ and $\Delta H°_{ads}$ were calculated and listed in Table 7. In both the systems, the nature of the dissolution process is endothermic as we can see from the positive signs of enthalpies $\Delta H°_{ads}$. The positive value of entropies $\Delta S°_{ads}$ in the presence of 50% *CSP* indicate that the inhibitor molecules are adsorbed onto the carbon steel surface. This can be obtaind by the formation of activated complex and more fixation of the system during the process [9-22].

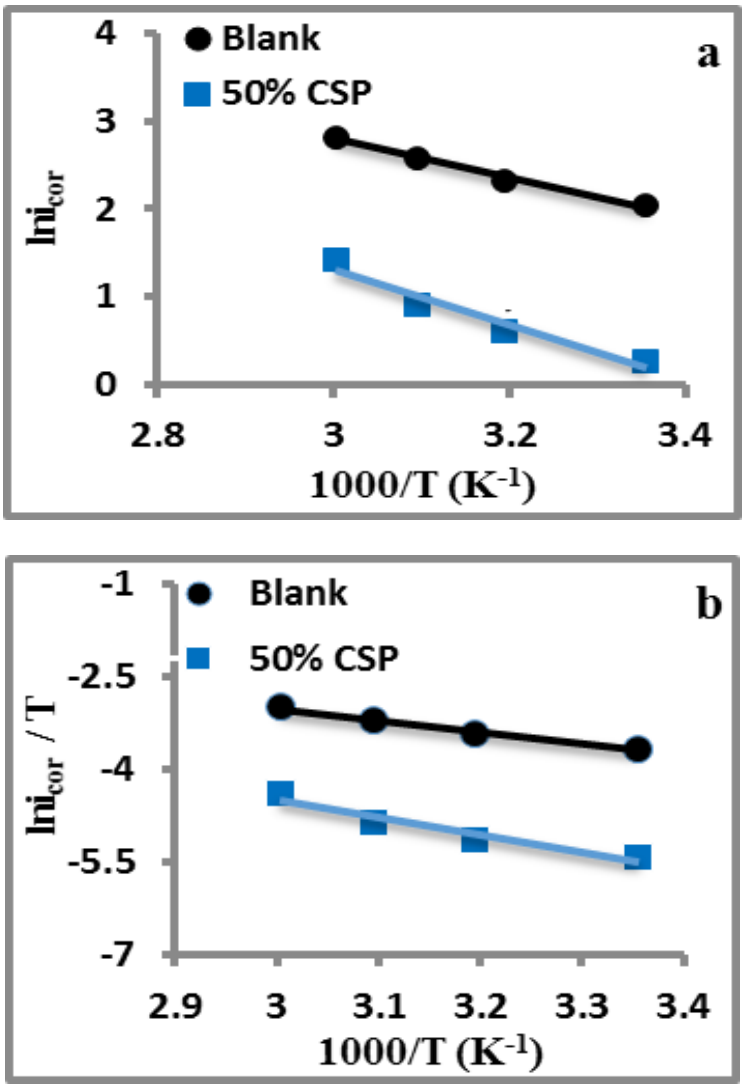

Figure. 7. (a) Arrhenius plots and (b) transition state plots for carbon steel in 1 M HCl with and without of 50% *CSP* extract.

Table 7. Thermodynamic activation parameters for Carbon Steel in 1M HCl with and without 50% of CSP extract.

Medium	E_{ads} (KJ)	$\Delta H°_{ads}$ (KJ/mol)	$\Delta S°_{ads}$ (KJ/mol K)
Blank	18.439	15.825	-175.122
CSP extract	25.829	23.215	-165.318

5. CONCLUSION

- The results obtained from the potentiodynamic polarization and EIS measurements demonstrated that the *CSP* extract acts as an effective inhibitor of carbon steel corrosion in 1 M HCl.
- Inhibition efficiency increases with the increase in the concentration of *CSP*, but decreases with rise in temperature.
- The adsorption of *CSP* on the carbon steel surface from 1 M HCl follows the Langmuir adsorption isotherm.
- The calculated values of $\Delta G°_{ads}$, E_a, $\Delta H°_{ads}$, and $\Delta S°_{ads}$ revealed that the adsorption process are spontaneous and endothermic, and the inhibitor molecules were adsorbed on the metal surface through mixed adsorption (physical and chemical adsorption).
- Consequently, all the results show that the *CSP* extract can act as an inhibitor against the corrosion of carbon steel in the HCl medium.

References

1. V. Torres, R. Amado, C. de Sa, T.L. Fernandez, C. da Silva Riehl, A. Torres and E. D'Elia, *Corrosion Science*, 53 (2011) 2385.
2. M. Majeed, A. Sultan and H. Al-Sahlanee, *Journal of Chemical and Pharmaceutical Research*, 5 (2013) 1297.
3. A. Sharmila, A. Prema and P. Sahayaraj, *Journal of Chemistry*, 3 (2010) 74.
4. N. Odewunmi, S. Umoren and Z. Gasem, *Journal of Industrial and Engineering Chemistry*, 21 (2015) 239.
5. M. Lebrini, F. Robert. A. Lecante and C. Roos, *Corrosion Science*, 53 (2011) 687.
6. P. Roy, P. Karfa, U. Adhikari and D. Sukul, *Corrosion Science*, 88 (2014) 246.
7. L. Li, X. Zhang, J. Lei, J. He, S. Zhang and F. Pan, *Corrosion Science*, 63 (2012) 82.
8. A.Fouda, S. Etaiw and W. Elnggar, *Int. J. Electrochem. Sci*., 9 (2014) 4866.
9. H. Zarrok, A. Zarrouk, R. Salghi, M. Assouag, B. Hammouti, H. Oudda, S. Boukhris, S. Al Deyab and I. Warad, *Der Pharmacia Lettre*, 5 (2013) 43.
10. A. Singh, V. Singh and M. Quraishi, *Arab J Sci Eng*., 38 (2013) 85.
11. M. Lebrini, F. Robert and C. Roos, *Int. J. Electrochem. Sci.* 5 (2010) 1698.

12. V. Rajeswaria, D. Kesavanb, M. Gopiramanc, P. Viswanathamurthia, K. Poonkuzhalid and T. Palvannand, *Applied Surface Science*, 314 (2014) 537.
13. A. Fouda, G. Elewady, K. Shalabi and S. Habouba, *International Journal of Advanced Reasearch*, 2 (2014) 817.
14. N. Lahhit; A. Bouyanzer; J. Desjobert; B. Hammouti, R. Salghi, J. Costa, C. Jama, F. Bentiss and L. Majidi, *Portugaliae Electrochemica Acta*, 29 (2011) 127.
15. A. Zadeh, I. Danaee and M. Maddahy, *J. Mater. Sci. Technol*., 29 (2013) 884.
16. N. Labjar, M. Lebrini, F. Bentiss, N. Chihib, S. Hajjaji and C. Jama, *Materials Chemistry and Physics*, 119 (2010) 330.
17. N. Negm, M. Zaki, M. Said and S. Morsy, *Corrosion Science*, 53 (2011) 4233.
18. A. El Bribri, M. Tabyaoui, B. Tabyaoui, H. El Attari and F. Bentiss, *Materials Chemistry and Physics*, 141 (2013) 240.
19. A. Lecante, F. Robert, P. A. Blandinieres and C. Roos, *Current Applied Physics*, 11 (2011) 714.
20. G. Golestani, M. Shahidi and D. Ghazanfari, *Applied Surface Science*, 308 (2014) 347.
21. A. Hamdy and N. El-Gendy, *Egyptian Journal of Petroleum*, 22 (2013) 17.
22. M. Majeed, A. Sultan and H. Al-Sahlanee, *J. Chem. Pharm. Res*., 6 (2014) 996.

© 2016 The Authors. Published by ESG (www.electrochemsci.org). This article is an open access article distributed under the terms and conditions of the Creative Commons Attribution license (http://creativecommons.org/licenses/by/4.0/).